

**Resonant Raman spectroscopy of armchair carbon nanotubes: Absence of broad  $G^-$  feature**E. H. Házroz,<sup>1,2</sup> J. G. Duque,<sup>3,4</sup> W. D. Rice,<sup>1,2,5</sup> C. G. Densmore,<sup>3</sup> J. Kono,<sup>1,2,5,\*</sup> and S. K. Doorn<sup>4,†</sup><sup>1</sup>*Department of Electrical and Computer Engineering, Rice University, Houston, Texas 77005, USA*<sup>2</sup>*The Richard E. Smalley Institute for Nanoscale Science and Technology, Rice University, Houston, Texas 77005, USA*<sup>3</sup>*Chemistry Division, Los Alamos National Laboratory, Los Alamos, New Mexico 87545, USA*<sup>4</sup>*Center for Integrated Nanotechnologies, Los Alamos National Laboratory, Los Alamos, New Mexico 87545, USA*<sup>5</sup>*Department of Physics and Astronomy, Rice University, Houston, Texas 77005, USA*

(Received 22 July 2011; published 9 September 2011)

The appearance of a broad Raman peak at  $\sim 1550\text{ cm}^{-1}$  ( $G^-$  peak) in carbon nanotubes has been conventionally attributed to the presence of metallic nanotubes. Here, we present wavelength-dependent resonant Raman measurements on macroscopic nanotube ensembles enriched in armchair species prepared via density gradient ultracentrifugation. Our data clearly show that the broad  $G^-$  mode is absent for armchair structures and appears only when the excitation laser is resonant with non-armchair “metals.” Due to the large number ( $\sim 10^{10}$ ) of nanotubes across several armchair species probed, our work firmly establishes a general correlation between the  $G$ -band line shape and nanotube structure.

DOI: [10.1103/PhysRevB.84.121403](https://doi.org/10.1103/PhysRevB.84.121403)

PACS number(s): 78.67.Ch, 73.22.-f, 78.30.Na

Armchair carbon nanotubes have a distinguished status among all the members, or species, of the single-walled carbon nanotube (SWNT) family. Being the only truly gapless species in the family, they are expected to exhibit some of the unusual properties characteristic of one-dimensional (1D) metals.<sup>1</sup> While strong electron-electron interactions can lead to the formation of Luttinger liquid states, strong electron-phonon interactions can renormalize phonon frequencies and lifetimes (Kohn anomalies) and induce Peierls lattice instabilities, especially in small-diameter nanotubes.<sup>2-5</sup> At the same time, as exceptionally conductive wires,<sup>6</sup> they are promising for a variety of electronic applications.

Recently, much progress has been made<sup>2,7-9</sup> in understanding electron-phonon interactions and their consequences in Raman spectra of “metallic” SWNTs, in which the chiral indices  $(n, m)$  satisfy  $\nu \equiv (n - m) \bmod 3 = 0$ , as opposed to semiconducting SWNTs, for which  $\nu = \pm 1$ . Note that, while armchair ( $n = m$ ) tubes are metallic (gapless), non-armchair ( $n \neq m$ )  $\nu = 0$  tubes have curvature-induced band gaps.<sup>10,11</sup> Of particular interest is the  $G$ -band, a Raman-active optical phonon feature due to the in-plane C-C stretching mode of  $sp^2$ -hybridized carbon. In SWNTs, the  $G$ -band is split in two, the  $G^+$  and  $G^-$  peaks, due to the curvature-induced inequality of the two bond-displacement directions. For  $\nu = 0$  tubes, the higher-frequency mode ( $G^+$ ) is a narrow Lorentzian peak, while the lower-frequency mode ( $G^-$ ) is extremely broad. Earlier theoretical studies described this broad feature as a Breit-Wigner-Fano line shape due to the coupling of phonons with an electronic continuum<sup>12</sup> or low-frequency plasmons,<sup>13</sup> but there is now accumulating consensus that the broad  $G^-$  peak is a softened and broadened longitudinal optical (LO) phonon feature, a hallmark of Kohn anomalies.<sup>2,7-9,14-16</sup> Through either scenario, this broad  $G^-$  peak has conventionally been known to be a “metallic” feature, indicating the presence of metallic tubes.

Here, we present detailed wavelength-dependent Raman scattering measurements on a macroscopic ensemble of SWNTs enriched in armchair (or  $n = m$ ) nanotubes produced via density gradient ultracentrifugation.<sup>17</sup> Our  $G$ -band spectra

clearly show that the broad  $G^-$  mode is absent for armchair structures and only occurs for non-armchair (or  $n \neq m$ ) “metallic” nanotubes. Ironically, the conventional method for identifying metallic nanotubes by observing a broad  $G^-$  peak does not apply to the only truly metallic species, i.e., armchair nanotubes. This supports an earlier conclusion based on a small number of single-tube measurements<sup>15,18</sup> and negates other claims that armchair nanotubes also show a broad  $G^-$  feature.<sup>19,20</sup> This lack of agreement between these and previous experimental and theoretical efforts has resulted in some confusion within the nanotube community as to the phenomenological origin of this Raman feature. Our results firmly establish a general correlation between the  $G$ -band line shape and nanotube structure on a macroscopic scale due to the sampling of a statistically significant number ( $\sim 10^{10}$ ) of nanotubes across multiple armchair species, eliminating any ambiguity.

Density gradient ultracentrifugation (DGU), using our previously reported procedures, was employed to create armchair-enriched (AE-SWNT)<sup>17</sup> and “metal”-enriched (ME-SWNT)<sup>21</sup> aqueous surfactant suspensions of SWNTs, synthesized by the high-pressure carbon monoxide method (HiPco) at Rice University. The ME-SWNT was a mixed ensemble containing both armchair and non-armchair (narrow-gap)  $\nu = 0$  “metallic” tubes. All DGU samples were dialyzed into surfactant and water to remove the density gradient medium. The as-produced HiPco SWNT reference sample (AP-SWNT) was produced using the standard ultracentrifugation technique in 1% (wt/vol) sodium deoxycholate (water).<sup>22,23</sup>

Resonant cw Raman spectroscopy was performed in a backscattering geometry with frequency-doubled Ti:sapphire laser excitation (440–500 nm), Ar<sup>+</sup> ion laser discrete lines (501.7 and 514.5 nm), and tunable dye laser excitation [with Rhodamine 6G (552–615 nm) and Kiton Red (610–680 nm)]. The laser power at the sample was maintained at 25 mW with a spot size of  $\sim 300\ \mu\text{m}$ . Individual Stokes-shift spectra were obtained at 5-min integrations using a CCD camera mounted on a triple monochromator. The nonresonant Raman spectrum of 4-acetamidophenol, acquired at each excitation wavelength,

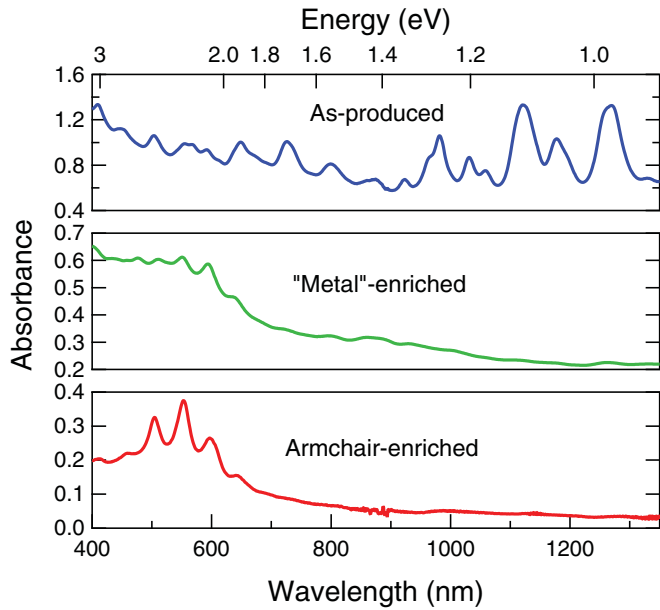


FIG. 1. (Color online) Optical absorption of the three nanotube suspensions studied: as-produced (AP-SWNT, blue), “metal”-enriched (ME-SWNT, green), and armchair-enriched (AE-SWNT, red). Note ME-SWNT and AE-SWNT show significant suppression of features due to  $\nu = \pm 1$  SWNTs as compared to AP-SWNT, indicating the elimination of  $\nu = \pm 1$  species and hence  $\nu = 0$  enrichment by the DGU process.

was used for both frequency calibration and for correcting intensities for instrument response. All data were taken at room temperature and ambient pressure.

Figure 1 shows absorption spectra of the three HiPco SWNT samples. The AP-SWNT sample (top, blue trace) displays all the typically observed features corresponding to the first ( $E_{11}^S$ , 850–1600 nm) and second ( $E_{22}^S$ , 570–850 nm) interband transitions of  $\nu = \pm 1$  tubes and the first ( $E_{11}^M$ , 400–650 nm) interband transitions of  $\nu = 0$  tubes. Based on absorption peak area estimates, this sample contains  $\sim 40\%$   $\nu = 0$  nanotubes,<sup>17</sup> which agrees reasonably well with the expected value of 34% from the number of possible  $(n, m)$  species contained within the diameter range (0.6–1.4 nm) of this particular material. After DGU, however, a significant suppression of  $\nu = \pm 1$  features (650–1350 nm) is observed in both the ME-SWNT (middle, green trace) and AE-SWNT (bottom, red trace) samples with  $\nu = 0$  purity estimates around 90% and 98%, respectively. While both DGU samples are strongly enriched in  $\nu = 0$  tubes, previous Raman studies based on radial breathing mode (RBM) intensities show that ME-SWNT samples are a *bulk* enrichment of all  $\nu = 0$  species<sup>21</sup> whereas AE-SWNT samples are chiral-angle-selective toward armchairs ( $n = m$ ).<sup>17</sup> This accounts for the sharper absorption features observed in the AE-SWNT sample due to the sizable reduction of the number of overlapping peaks from the various  $\nu = 0$  species.

Figure 2(a) shows Raman spectra for both the RBM and  $G$ -band ranges for all SWNT samples, collected at 552-nm excitation. Comparing to existing experimental and theoretical Kataura plots in the literature, this wavelength primarily resonates with members of the  $(2n + m) = 24$  family [(8,8) and (10,4)] as well as some small-diameter  $\nu = 1$  species

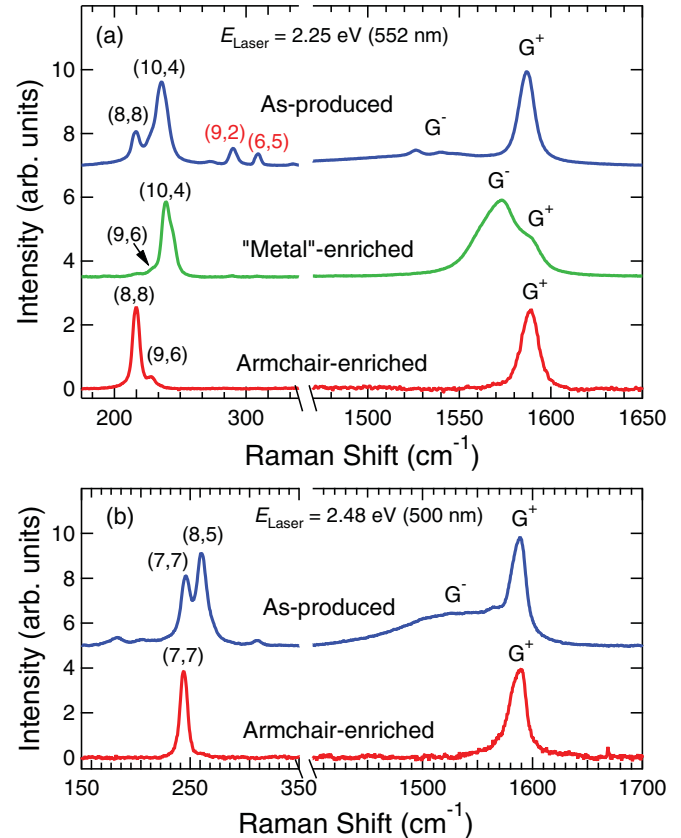


FIG. 2. (Color online) Raman spectra of RBM and  $G$  band for AP-SWNT, ME-SWNT, and AE-SWNT samples taken at excitation wavelengths (a) 552 nm and (b) 500 nm where SWNTs from families  $(2n + m) = 24$  and 21, respectively, are primarily probed. The appearance of the broad  $G^-$  feature corresponds to resonance with non-armchair species such as (10,4) in ME-SWNT in (a) and (8,5) in AP-SWNT in (b). In the case of sole resonance with armchair species [(8,8) and (7,7)], a single and narrow  $G^+$  peak is observed.

[(9,2) and (6,5)]. Examining the RBM region first, it is clearly confirmed that indeed the ME-SWNT (green trace) and AE-SWNT (red trace) samples are enriched in  $\nu = 0$  tubes while the AP-SWNT sample (blue trace) contains a mixture of  $\nu = 1$  and  $\nu = 0$  species. Furthermore, the ME-SWNT sample contains most of the members of family 24, whereas the AE-SWNT sample contains only the (8,8) armchair species with a very small amount of (9,6).

In the corresponding  $G$ -band region for the AP-SWNT (blue trace) in Fig. 2(a), we observe a  $G$ -band line shape typical of resonance with  $\nu = 1$  species such as (9,2) and (6,5), because the intensity of the  $G^+$  peak for  $\nu = \pm 1$  tubes is markedly stronger than that for  $\nu = 0$  tubes.<sup>24,25</sup> With the removal of the  $\nu = \pm 1$  impurities, the ME-SWNT sample displays a  $G$ -band line shape typically ascribed in the literature to the presence of only metallic nanotubes with the notably broad  $G^-$  component [green trace in Fig. 2(a)]. However, the AE-SWNT sample, also free of  $\nu = \pm 1$  impurities, shows a completely different  $G$ -band line shape consisting of only a single and narrow  $G^+$  component [red trace in Fig. 2(a)]. Such a large difference in  $G$ -band line shape between these two samples suggests a significant  $(n, m)$  dependence of the

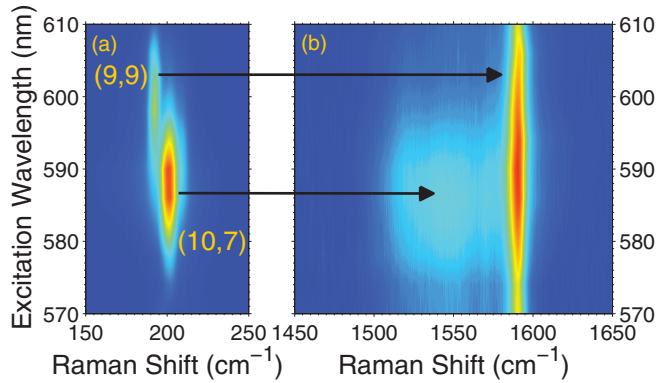


FIG. 3. (Color online) Raman intensity for AE-SWNT taken as a function of Raman shift and excitation wavelength for family  $(2n + m) = 27$ . (a) RBM region where two clear RBMs due to the (9,9) and (10,7) are observed. (b) Corresponding  $G$ -band region where only the  $G^+$  peak is observed when resonating primarily with the (9,9) and the appearance of the broad  $G^-$  coincides with the maximum of the (10,7) RBM.

$G^-$  feature. In fact, when taken together with the RBM spectrum for the ME-SWNT sample, a correlation between the appearance of small chiral-angle (or zigzag-like)  $\nu = 0$  species and that of the  $G^-$  peak is evident. Furthermore, this peak becomes absent at resonance with armchair tubes.

Examining another  $\nu = 0$  family,  $(2n + m) = 21$ , we see a similar trend. In Fig. 2(b), we present resonant Raman spectra of the RBM and  $G$ -band ranges for the AP-SWNT and AE-SWNT samples taken at 500-nm excitation. At this wavelength, both samples are spectrally isolated from any  $\nu = \pm 1$  impurities, and, as such, only resonance with the  $\nu = 0$  tubes occurs. AP-SWNT displays resonance with only two species, (8,5) and (7,7). Correspondingly, we observe the broad  $G^-$  feature and a narrow  $G^+$  component. In contrast, AE-SWNT resonates singly with the armchair species (7,7) and again displays a single, narrow  $G^+$  peak as AE-SWNT in Fig. 2(a).

To further study the relationship between the appearance of the broad  $G^-$  peak and  $(n,m)$  composition, we examined another isolated  $\nu = 0$  family,  $(2n + m) = 27$ . Figure 3 shows a contour plot of Raman intensity of the AE-SWNT sample for the RBM and  $G$ -band regions over excitation wavelengths of 570–610 nm. In Fig. 3(a), we see only two RBMs, from (9,9) and (10,7), again reflecting enrichment toward armchair-like species. The corresponding  $G$ -band [Fig. 3(b)] shows only a single  $G^+$  peak centered at  $\sim 1590 \text{ cm}^{-1}$  at the longest excitation wavelengths ( $\sim 610 \text{ nm}$ ) coinciding primarily with resonance of the (9,9) RBM. As the wavelength is decreased, a broad  $G^-$  peak appears in addition to the  $G^+$  peak. This broad  $G^-$  peak, centered at  $\sim 1550 \text{ cm}^{-1}$ , reaches a maximum in intensity at  $\sim 587 \text{ nm}$ , which coincides with the RBM resonance maximum of the (10,7) and its absence with pure resonance with the (9,9) point out a clear correlation between  $(n,m)$  chirality and  $G$ -band line shape. Namely, the broad  $G^-$  peak appears only in the presence of non-armchair  $\nu = 0$  nanotube species, and  $(n,n)$  armchair species consist of only one single, narrow peak.

Finally, Fig. 4 shows selected Raman spectra of the (7,7), (8,8), (9,9), and (10,10) armchair families taken at 500-, 552-,

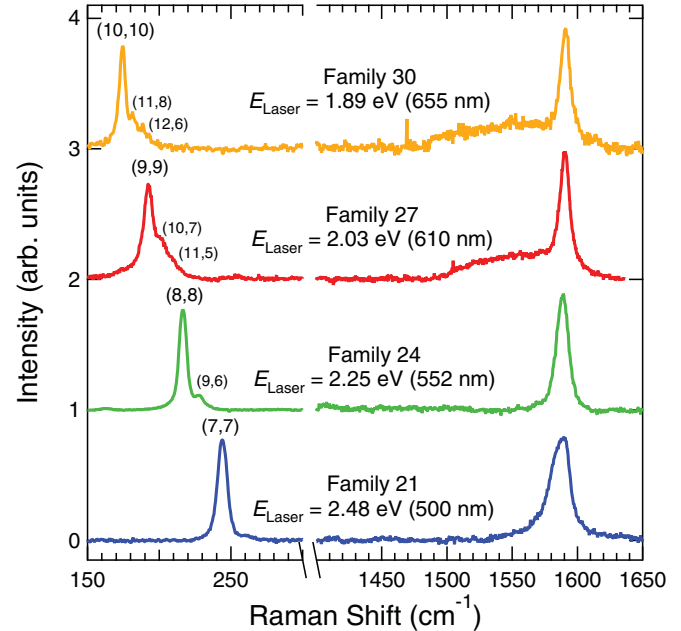


FIG. 4. (Color online) Selected resonant Raman spectra for AE-SWNT taken at excitation wavelengths 655-, 610-, 552-, and 500-nm, where resonance primarily occurs with armchairs (10,10), (9,9), (8,8), and (7,7), respectively. In each case, the  $G$ -band reflects contribution mainly from the  $G^+$  peak only.

610-, and 655-nm excitations, respectively, for the AE-SWNT sample. These wavelengths are close to the general resonance maxima for each respective family. Data taken across a diameter range of 0.96–1.38 nm shown here clearly demonstrates that the appearance and dominance of a single  $G^+$  feature is a general result and indicator for the predominance of armchair species. The observation of the weak  $G^-$  peak at 610 and 655 nm represents the non-negligible but small contribution of residual non-armchair  $\nu = 0$  impurities [(10,7) and (11,8)] and a qualitative measure of the larger Raman cross section such species have as compared to armchair tubes.<sup>25</sup>

Based on the aforementioned results, we attribute the narrow  $G^+$  component observed during resonance with all  $\nu = 0$  species to the transverse optical (TO) phonon mode and the broad  $G^-$  component observed only with  $\nu = 0$ , non-armchair species to the LO phonon mode arising from phonon softening due to Kohn anomaly.<sup>2,7–9,14–16</sup> The absence of the LO phonon feature for armchair tubes is consistent with some theoretical studies (e.g., Refs. 2 and 26), i.e., it is *not* Raman active in armchairs (although this still does not eliminate the presence of a Kohn anomaly—only its Raman activity), while it is inconsistent with more recent theories.<sup>19,20</sup>

Single-tube Raman studies of armchairs have observed both the absence<sup>15,18,27</sup> and presence<sup>20</sup> of a broad  $G^-$  feature in freestanding and substrate-supported SWNTs, respectively. The consistency of freestanding, single-tube data in Refs. 15, 18, and 27, where  $(n,m)$  is assigned independently by other means, with our own data is a direct result of the largely nonperturbative environment surrounding our surfactant-suspended tubes. Thus, the disagreement among single-tube results on the more commonly used substrate-supported samples stems from the sensitivity of the  $G$ -band to charge transfer from intentional

gating<sup>14,15</sup> and environmental effects that can induce a localization of electron density in the nanotube  $\pi$  electron cloud.<sup>28,29</sup> As a result, great care must be taken in generalizing the observed  $G$ -band structure at the single-tube level for a given chiral species because of this sensitivity and that only a few nanotube examples are typically sampled in an experiment.

In contrast, the lack of broad LO phonon for armchairs observed here is a result of our macroscopic ensembles containing  $\sim 10^{10}$  nanotubes per chirality in combination with the spectral isolation of each species. Any tube-to-tube variations measured are essentially removed due to this large statistical sampling, and the resulting recorded spectrum represents the average response for each chirality. Since this study spans four consecutive armchair species, three of which have not been previously measured in the literature and all of which are in the small-diameter limit, generalization of the absence of a broad LO peak to all armchair nanotubes is appropriate and justifiable. Furthermore, a refinement in the specificity of the use of the broad  $G^-$  peak as a “metallic” signature can be made where its appearance is indicative of resonance with non-armchair,  $\nu = 0$  species. The appearance of only a single, narrow  $G^+$  in SWNT ensembles enriched in “metallic” species signifies pure resonance with spectrally isolated armchair species. Given the scope and breadth of this study, we believe

the confusion amongst researchers regarding the  $G$ -band and metallic nanotubes is finally and convincingly resolved.

In conclusion, using resonant Raman measurements of macroscopic ensembles of  $\nu = 0$  enriched SWNT samples, we have demonstrated that the appearance of a broad  $G^-$  peak is due to the presence of non-armchair “metallic” tubes. More importantly, the  $G$ -band of armchair tubes consists of a single, narrow  $G^+$  component and serves as a further diagnostic for their identification. Because of the large statistical sampling presented here, these results are generalizable to all  $\nu = 0$  nanotubes. Finally, this study demonstrates the ability of using specialized, enriched samples such as these to extract meaningful and definitive information about single chiralities from a macroscopic scale, enabling future studies beyond the experimental limitations of the single-tube level.

This work was supported by the DOE/BES through Grant No. DEFG02-06ER46308, the Robert A. Welch Foundation through Grant No. C-1509, the Air Force Research Laboratories under Contract No. FA8650-05-D-5807, and the LANL LDRD Program. This work was performed in part at the Center for Integrated Nanotechnologies, a US Department of Energy, Office of Basic Energy Sciences user facility. We thank C. Kittrell, R. H. Hauge, and R. Saito for useful discussions.

\*kono@rice.edu

†skdoorn@lanl.gov

<sup>1</sup>T. Giamarchi, *Quantum Physics in One Dimension* (Oxford University Press, Oxford, UK, 2004).

<sup>2</sup>O. Dubay, G. Kresse, and H. Kuzmany, *Phys. Rev. Lett.* **88**, 235506 (2002).

<sup>3</sup>K.-P. Bohnen, R. Heid, H. J. Liu, and C. T. Chan, *Phys. Rev. Lett.* **93**, 245501 (2004).

<sup>4</sup>D. Connétable, G. M. Rignanese, J. C. Charlier, and X. Blase, *Phys. Rev. Lett.* **94**, 015503 (2005).

<sup>5</sup>R. Barnett, E. Demler, and E. Kaxiras, *Phys. Rev. B* **71**, 035429 (2005).

<sup>6</sup>Z. Yao, C. L. Kane, and C. Dekker, *Phys. Rev. Lett.* **84**, 2941 (2000).

<sup>7</sup>M. Lazzeri, S. Piscanec, F. Mauri, A. C. Ferrari, and J. Robertson, *Phys. Rev. B* **73**, 155426 (2006).

<sup>8</sup>K. Ishikawa and T. Ando, *J. Phys. Soc. Jpn.* **75**, 084713 (2006).

<sup>9</sup>S. Piscanec, M. Lazzeri, J. Robertson, A. C. Ferrari, and F. Mauri, *Phys. Rev. B* **75**, 035427 (2007).

<sup>10</sup>N. Hamada, S. I. Sawada, and A. Oshiyama, *Phys. Rev. Lett.* **68**, 1579 (1992).

<sup>11</sup>C. L. Kane and E. J. Mele, *Phys. Rev. Lett.* **78**, 1932 (1997).

<sup>12</sup>S. D. M. Brown, A. Jorio, P. Corio, M. S. Dresselhaus, G. Dresselhaus, R. Saito, and K. Kneipp, *Phys. Rev. B* **63**, 155414 (2001).

<sup>13</sup>K. Kempa, *Phys. Rev. B* **66**, 195406 (2002).

<sup>14</sup>K. T. Nguyen, A. Gaur, and M. Shim, *Phys. Rev. Lett.* **98**, 145504 (2007).

<sup>15</sup>Y. Wu, J. Maultzsch, E. Knoesel, B. Chandra, M. Huang, M. Y. Sfeir, L. E. Brus, J. Hone, and T. F. Heinz, *Phys. Rev. Lett.* **99**, 027402 (2007).

<sup>16</sup>H. Farhat, H. Son, G. G. Samsonidze, S. Reich, M. S. Dresselhaus, and J. Kong, *Phys. Rev. Lett.* **99**, 145506 (2007).

<sup>17</sup>E. H. Hároz, W. D. Rice, B. Y. Lu, S. Ghosh, R. H. Hauge, R. B. Weisman, S. K. Doorn, and J. Kono, *ACS Nano* **4**, 1955 (2010).

<sup>18</sup>T. Michel, M. Paillet, D. Nakabayashi, M. Picher, V. Jourdain, and J. C. Meyer, A. A. Zahab, and J. L. Sauvajol, *Phys. Rev. B* **80**, 245416 (2009).

<sup>19</sup>K. I. Sasaki, R. Saito, G. Dresselhaus, M. S. Dresselhaus, H. Farhat, J. Kong, *Phys. Rev. B* **77**, 245441 (2008).

<sup>20</sup>J. S. Park, K. Sasaki, R. Saito, W. Izumida, M. Kalbac, H. Farhat, G. Dresselhaus, and M. S. Dresselhaus, *Phys. Rev. B* **80**, 081402 (2009).

<sup>21</sup>S. Niyogi, C. G. Densmore, and S. K. Doorn, *J. Am. Chem. Soc.* **131**, 1144 (2009).

<sup>22</sup>M. J. O’Connell, S. M. Bachilo, C. B. Huffman, V. C. Moore, M. S. Strano, E. H. Haroz, K. L. Rialon, P. J. Boul, W. H. Noon, C. Kittrell, J. Ma, R. H. Hauge, R. B. Weisman, and R. E. Smalley, *Science* **297**, 593 (2002).

<sup>23</sup>J. G. Duque, A. N. G. Parra-Vasquez, N. Behabtu, M. J. Green, A. L. Higginbotham, B. K. Price, A. D. Leonard, H. K. Schmidt, B. Lounis, J. M. Tour, S. K. Doorn, L. Cognet, and M. Pasquali, *ACS Nano* **4**, 3063 (2010).

<sup>24</sup>M. Machón, S. Reich, and C. Thomsen, *Phys. Rev. B* **74**, 205423 (2006).

<sup>25</sup>J. Jiang, R. Saito, G. G. Samsonidze, A. Jorio, S. G. Chou, G. Dresselhaus, and M. S. Dresselhaus, *Phys. Rev. B* **75**, 035407 (2007).

<sup>26</sup>R. Saito, A. Jorio, J. H. Hafner, C. M. Lieber, M. Hunter, T. McClure, G. Dresselhaus, and M. S. Dresselhaus, *Phys. Rev. B* **64**, 085312 (2001).

<sup>27</sup>S. Berciaud, C. Voisin, H. Yan, B. Chandra, R. Caldwell, Y. Shan, L. E. Brus, J. Hone, and T. F. Heinz, *Phys. Rev. B* **81**, 041414(R) (2010).

<sup>28</sup>A. M. Rao, P. C. Eklund, S. Bandow, A. Thess, and R. E. Smalley, *Nature (London)* **388**, 257 (1997).

<sup>29</sup>M. Shim, A. Gaur, K. T. Nguyen, D. Abdula, and T. Ozel, *J. Phys. Chem. C* **112**, 13017 (2008).